High resolution travel time tomography

Yonadav Sudman, and Dan Kosloff, Tel-Aviv U. and Paradigm Geophysical*

Summary

The velocity and interface depth determination is one of the most important tasks of exploration seismology. However the process of velocity-depth determination suffers from non-uniqueness of the solution. Traditional methods for imposing uniqueness suffer from loss of resolution and damping of the solution. This work presents an improvement to travel time tomography by using a wavelet expansion of the model parameters combined with Cauchy regularization. By this method we achieve a stable high resolution tomography which produces geologically plausible solutions. The method is tested on synthetic and field data.

Introduction

Subsurface geological models are usually parameterized as a set of velocities of the formations and the depths of the interfaces separating them. Excluding noise and data quality problems, the process of velocity-depth determination suffers from a spectral ambiguity resulting from lack of offsets in the data acquisition (Bickel, 1990; Bube et al., 1995; Kosloff and Sudman, 2002). Resolving this spectral ambiguity by improving data acquisition requires very large offsets (3 to 20 times the reflector depth) which are not realistic for exploration geophysics.

This research approaches the spectral ambiguity problem for reflection travel time tomography inversion (Farra and Madariaga, 1988; Kosloff et al., 1996). Traditionally, damped least squares combined with a coarse update grid, have been used to stabilize the solution. However, with this approach only very long wavelength features of the model are resolved, while short wavelength features are lost. Moreover, the damped inversion can only resolve a small part of the travel time error, thus requiring many tomography iterations to reach convergence.

This research suggests a new tomographic scheme based on a wavelet basis expansion of the solution combined with the Cauchy function regularization (Sacchi et al., 1998, Zwartjes and Hindriks, 2001). The fact that the wavelet transform contains both spatial (shift) and wave number (scale) representations of the tomographic updates (Mallat, 1999), allows for flexibilities in regularizing the solution by applying variances calculated from the background model (spatial) as well as a priory information regarding wave number content and noise. Moreover, wavelet representation of functions tends to be more compact (sparse) than their spatial representation. It appears that sparse solutions, which in our scheme are imposed by the Cauchy regularization, produce a more geologically feasible solution. The suggested scheme can be used with a fine update mesh with minimal damping to solve short wavelength phenomena and resolve most of the travel time errors.

Model descretization and wavelet transform

The tomography updates two types of parameters, the slowness of the formations and the depths of the interfaces which separate them. The model parameters are discretized in update points which are separated by the CRP step. Each update point includes the two parameters of slowness and interface depth. For achieving better convergence, the model parameters are subsequently transformed from slowness and depth to slowness and vertical time respectively (Kosloff et al., 1996).

After spatial descretization and linearization, the tomographic equations can be represented as a matrix product:

$$\mathbf{A}\delta\mathbf{m} = \delta\mathbf{t} \qquad (1$$

Where $\mathbf{A}$ is the tomography matrix, $\delta\mathbf{m}$ is the model perturbation vector and $\delta\mathbf{t}$ is the travel time error vector. Each row of the matrix $\mathbf{A}$ is of the form:

$$\mathbf{A}_k = \left[\mathbf{A}_k^{s,0}, \mathbf{A}_k^{s,1}, \mathbf{A}_k^{s,2}, ..., \mathbf{A}_k^{t_v,0}, \mathbf{A}_k^{t_v,1}, \mathbf{A}_k^{t_v,2}, ...\right].$$

Where $\mathbf{A}_k^{s,i}, \mathbf{A}_k^{t_v,i}$ symbolize entries in a row of $\mathbf{A}$ that corresponds to slowness and vertical time parameters, in the i^{th} formation, respectively. Similarly the update parameters are factored according to

$$\delta\mathbf{m} = [\delta\mathbf{m}^{s,0}, \delta\mathbf{m}^{s,1}, ..., \delta\mathbf{m}^{t_v,0}, \delta\mathbf{m}^{t_v,1}, ...].$$

Let $\mathbf{T}$ denote the operator of the wavelet transform. The expansion coefficients $\delta\tilde{\mathbf{m}}^{\alpha,i}$ for a given parameter type α, and formation number i are related to $\delta\mathbf{m}^{\alpha,i}$ by $\delta\tilde{\mathbf{m}}^{\alpha,i} = \mathbf{T}\delta\mathbf{m}^{\alpha,i}$. With this relation the tomography equation (1) can be rewritten for the expansion coefficients:

$$\tilde{\mathbf{A}}\delta\tilde{\mathbf{m}} = \delta\mathbf{t} \qquad (2$$

Where $\tilde{\mathbf{A}}_k^{\alpha,j} = \mathbf{A}_k^{\alpha,j}\mathbf{T}^{-1}$. By using this presentation of the tomography matrix the resulting inverted parameters will be in the wavelet domain.

The wavelet expansion of the parameters has two main advantages.

1. The wavelet coefficients of the model are separated to both their wave number content and spatial

location. This separation allows better regularization of the solution by a model variance that is generated for both wave number and location.

2. The wavelet representation of most of the functions is more compact (sparse) than the spatial one. Therefore, imposing sparseness of the solution may lead to a more geologically feasible solution.

Regularization by the Cauchy distribution

The Cauchy distribution function is of the functional form: $f(\delta\tilde{m}_k) \propto \left(1 + s\delta\tilde{m}_k^{\,2}\right)^{-1}$ (Sacchi et al., 1998, Zwartjes and Hindriks, 2001), hence the cost function for the tomography becomes:

$$\Phi = \left\| \mathbf{C}_D^{-1}\left(\delta\mathbf{t} - \tilde{\mathbf{A}}\delta\tilde{\mathbf{m}}\right)\right\| + \sum_{k=0}^{M-1} \ln\left(\frac{\sigma_m^{k\,2}}{1 + s\delta\tilde{m}_k^2}\right). \quad (3$$

$\delta\tilde{m}_k$ represent the expansion coefficient of the k[th] parameter (e.g. a slowness or vertical time update for a certain formation and CRP location), M is the number of model parameters, $C_D^{i,j} = \sigma_D^{i\,2}\delta_{ij}$ is the data covariance matrix, σ_D^i, σ_m^k are the data and model standard deviations respectively, and s is a scaling parameter. Equating the derivative of Φ, with respect to $\delta\tilde{m}_k$, to zero yields the following nonlinear equation system

$$\left(\boldsymbol{\Psi} + \tilde{\mathbf{A}}^T\mathbf{C}_D^{-1}\tilde{\mathbf{A}}\right)\delta\tilde{\mathbf{m}} = \tilde{\mathbf{A}}^T\mathbf{C}_D^{-1}\delta\mathbf{t} \quad (4$$

Where $\Psi^{i.j} = \frac{\sigma_m^{j\,2}}{\left(1 + s\delta\tilde{m}_j^2\right)}\delta_{ij}$ is the Cauchy regularizer. This equation system can be solved iteratively using the conjugate gradient method. This norm promotes sparse solutions compared to the standard Gaussian damped solutions.

Synthetic example

The synthetic survey geometry consists of 512 CMPs with a CMP increment of 25 m, and 30 offsets with an offset increment of 100 m, with a first offset of 100 m. The input CRP panels for the tomography were muted at about 1:1 reflector depth to offset ratio. The initial model includes three horizontal layers (Fig. 1, solid lines) with constant velocities of 2000 m/s, 2400 m/s and 3000 m/s, for the first second and third formation respectively. The "correct" model was created by applying a small anticlinal perturbation to the velocities of the two first formations, and a constant velocity shift of 80 m/s in the third formation, while preserving zero-offset times in the depth model. The input data was generated by CMP modeling from the "correct" model. The CMP gathers were subsequently migrated using the initial model. The input to the tomography included the initial model and CRP panels that were created from the migrated gathers (Kosloff et al., 1996).

Figure 1a compares the "correct" model (solid line) to the topographically reconstructed model (dotted line) when using Gaussian regularization with a fine update mesh size of 4 CRPs. As this Figure shows, especially in the third layer, there are locations where the topographically reconstructed model differs significantly from the correct model. Figure 1b presents a similar comparison for a coarser update mesh size of 25 CRPs. The tomographic reconstruction in this case is more stable than the one of the previous test. However, the small anticlinal features of the correct model were not reconstructed properly. Figure 1c compares the correct model to the topographically reconstructed model when using Cauchy regularization in the wavelet domain with a fine update grid size of 4 CRPs. The tomographic reconstruction in this case is significantly better than the two previous ones. Short wavelength features are reconstructed correctly without noticeable disturbances in the two first formations, and only a 20 m/s error in the third formation.

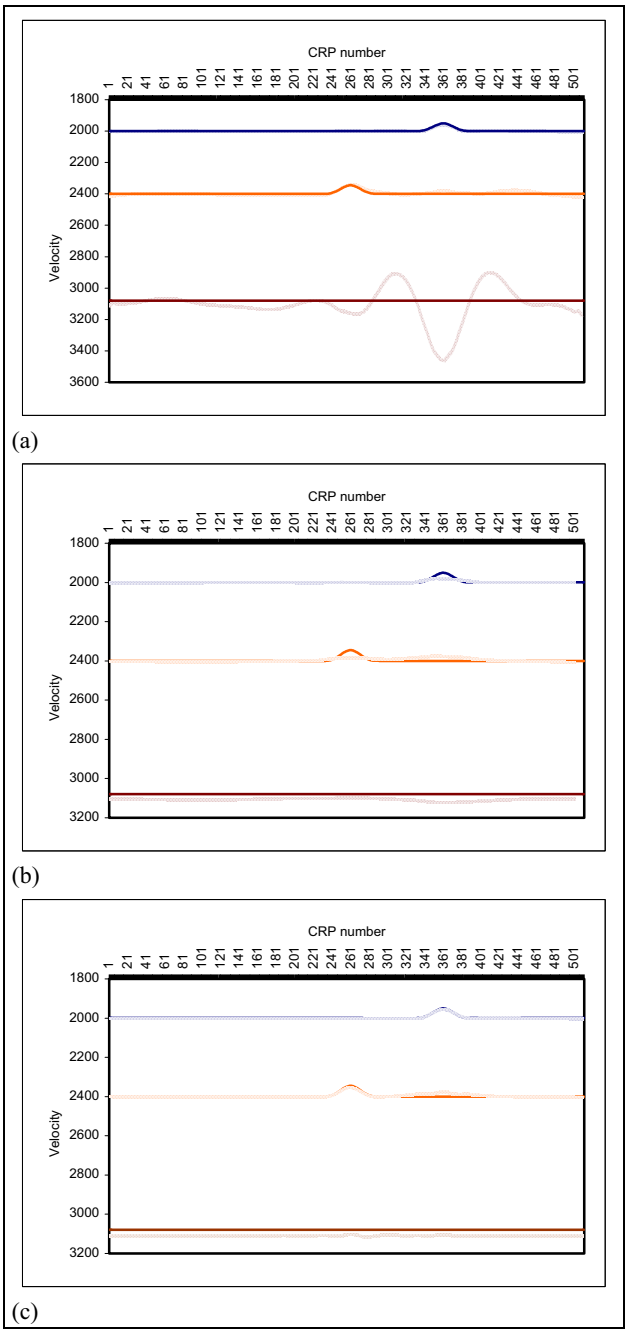

Fig. 1: Tomographic results (doted) compared to the "correct" model. a) Gaussian norm with fine update grid. b) Gaussian norm with coarse update grid. c) Cauchy regularization with fine update grid.

Field data example

The field data geometry consists of 256 CMPs with a CMP increment of 25 m, and an average fold of 57 offsets with an average offset increment of 80 m. The background model in this example includes three non-horizontal layers with laterally variant velocity and laterally invariant vertical gradient (Fig. 2 solid line). The vertical gradient serves only as a background model and the tomography updates only the initial velocity and depth. The data was migrated using the initial model followed by creation of CRP panels from the migrated gathers.

Figure 2a shows the depth migrated section using the initial model. Figure 2b presents the tomographic results using wavelet based tomography with Cauchy regularization and a fine update mesh spacing of 4 CRPs (doted line). Figure 2c shows the CRP panels before and after tomography. As figures 2b and 2c show the tomographically reconstructed model is stable and the CRP panels are corrected well with significantly higher semblance values.

Conclusions

We presented a tomographic scheme which is based on a wavelet expansion of the model parameters and Cauchy regularization. The results show that this method can reconstruct short wavelength perturbations better than the standard Gaussian damping. This research is important especially in cases where short wavelengths resolution is needed. Examples for such cases are locating overpressure zones or reconstructing small velocity anomalies in shallow layers.

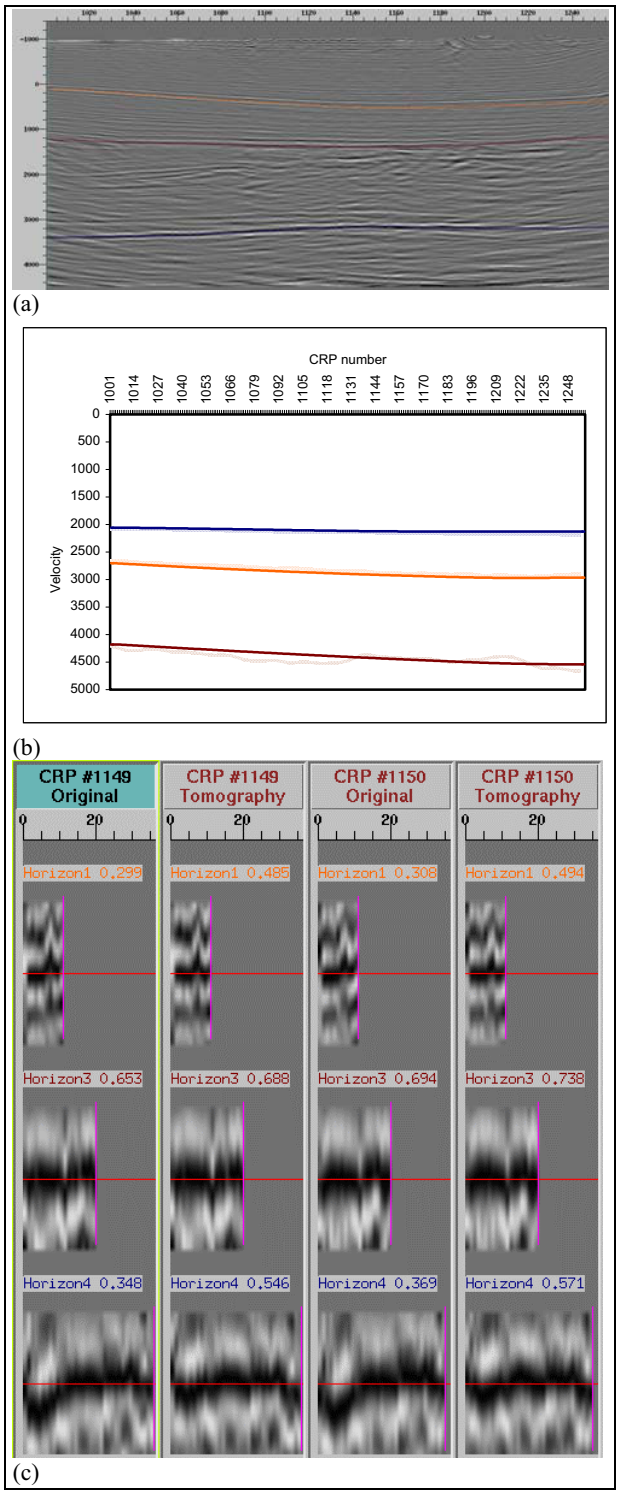

Fig. 2. (a) Depth migrated section. (b) Tomographic results (doted) compared to the initial model (solid) using the Cauchy norm. (c) CRP panels before and after tomography.

References

Bickel, S. H., 1990, Velocity-depth ambiguity of reflection travel times, Geophysics, 55, 266-278.

Bube, K.P., Langan, R.T., and Resnick, R., R., 1995. Theoretical and numerical issues in the determination of reflector depths in seismic reflection tomography. JGR VOL. 100. No. B7, 12449-12458.

Farra, V., and Madariaga, R., 1988, Nonlinear reflection tomography, Geophysics Journal. International, 95,135-147.

Kosloff, D., Sherwood, J., Koren, Z., Machet, E., and Falkovitz, Y., 1996, Velocity and interface depth determination by tomography of depth migrated gathers, Geophysics, 61, 1511-1523.

Kosloff, D., Sudman, Y., 2002, Uncertainty in determining interval velocities from surface reflection seismic data, Geophysics, in press.

Mallat, S., 1999, A wavelet tour of signal processing, Academic Press.

Zwartjes, P.M., Hindriks, 2001, C.O.H., Regularizing 3D data using Fourier reconstruction and sparse inversion, SEG Mtg., Exp. Abs., 1906-1909.